Loss determination in microsphere resonators by phase-shift cavity ring-down measurements

J. Barnes[1], B. Carver[1], J. M. Fraser[2], G. Gagliardi[3], H.-P. Loock[1*], Z. Tian[2], M.W.B. Wilson[2], S. Yam[4], O. Yastrubshak[2]

[1]*Department of Chemistry, Queen's University, Kingston, ON, K7L 3N6, Canada*
[2] *Department of Physics, Queen's University, Kingston, ON, K7L 3N6, Canada*
[3] Consiglio Nazionale delle Ricerche-Istituto Nazionale di Ottica Applicata (INOA), Pozzuoli (Naples), Italy
[4] *Department of Electrical and Computer Engineering, Queen's University, K7L 3N6, Canada*
[*]*Corresponding author: hploock@chem.queensu.ca*

Abstract: The optical loss of whispering gallery modes of resonantly excited microresonator spheres is determined by optical lifetime measurements. The phase-shift cavity ring-down technique is used to extract ring-down times and optical loss from the difference in amplitude modulation phase between the light entering the microresonator and light scattered from the microresonator. In addition, the phase lag of the light exiting the waveguide, which was used to couple light into the resonator, was measured. The intensity and phase measurements were fully described by a model that assumed interference of the cavity modes with the light propagating in the waveguide.

OCIS codes: (230.3990) Micro-optical devices; (230.5750) Resonators.

References and links

1. A. M. Armani, D. K. Armani, B. Min, K. J. Vahala, and S. M. Spillane, "Ultra-high-Q microcavity operation in H_2O and D_2O," Appl. Phys. Lett. **87**, 151118 (2005).
2. R. W. Boyd and J. E. Heebner, "Sensitive disk resonator photonic biosensor," Appl. Opt. **40**, 5742 (2001).
3. C. Chao and L. J. Guo, "Polymer microring resonators fabricated by nanoimprint technique," J. Vac. Sci. Technol. B **20**, 2862 (2002).
4. E. Krioukov, D. J. W. Klunder, A. Driessen, J. Greve, and C. Otto, "Integrated optical microcavities for enhanced evanescent-wave spectroscopy," Opt. Lett. **27**, 1504 (2002).
5. T. Ling and L. J. Guo, "A unique resonance mode observed in a prism-coupled micro-tube resonator sensor with superior index sensitivity," Opt. Express **15**, 17424 (2007).
6. D. W. Vernooy, V. S. Ilchenko, H. Mabuchi, E. W. Streed, and H. J. Kimble, "High-Q measurements of fused-silica microspheres in the near infrared," Opt. Lett. **23**, 247 (1998).
7. I. M. White, H. Oveys, and X. Fan, "Liquid-core optical ring-resonator sensors," Opt. Lett. **31**, 1319 (2008).
8. T. J. Kippenberg, SpillaneS.M., D. K. Armani, and K. J. Vahala, "Ultralow-threshold microcavity Raman laser on a microelectronic chip," Opt. Lett. **29**, 1224 (2004).
9. S. I. Shopova, G. Farca, A. T. Rosenberger, W. M. S. Wickramanayake, and N. A. Kotov, "Microsphere whispering-gallery-mode laser using HgTe quantum dots," Appl. Phys. Lett. **85**, 6101 (2004).
10. M. Cai, G. Hunziker, and K. Vahala, "Fiber-Optic Add-Drop Device Based on a Silica Microsphere Whispering Gallery Mode System," IEEE Photon. Technol. Lett **11**, 686 (1999).
11. S. Arnold, M. Khoshsima, I. Teraoka, S. Holler, and F. Vollmer, "Shift of whispering-gallery modes in microspheres by protein adsorption," Opt. Lett. **28**, 272 (2003).
12. G. Farca, S. I. Shopova, and A. T. Rosenberger, "Cavity-enhanced laser absorption spectroscopy using microresonator whispering-gallery modes," Opt. Express **15**, 17443 (2007).
13. A. M. Armani and K. J. Vahala, "Heavy water detection using ultra-high-Q microcavities," Opt. Lett. **31**, 1896 (2006).
14. A. T. Rosenberger, "Analysis of whispering-gallery microcavity-enhanced chemical absorption sensors," Opt. Express **15**, 12959 (2007).
15. K. J. Vahala, "Optical microcavities," Nature **424**, 839 (2003).
16. G. Berden, R. Peeters, and G. Meijer, "Cavity ring-down spectroscopy: Experimental schemes and applications," Int. Rev. Phys. Chem. **19**, 565 (2000).
17. A. C. R. Pipino, "Ultrasensitive surface spectroscopy with a miniature optical resonator," Phys. Rev. Lett. **83**, 3093 (1999).
18. R. S. Brown, I. Kozin, Z. Tong, R. D. Oleschuk, and H.-P. Loock, "Fiber-loop ring-down spectroscopy," J. Chem. Phys. **117**, 10444 (2002).

#95586 - $15.00 USD Received 30 Apr 2008; revised 8 Aug 2008; accepted 11 Aug 2008; published 13 Aug 2008

19. D. K. Armani, T. J. Kippenberg, S. M. Spillane, and K. J. Vahala, "Ultra-high-Q toroid microcavity on a chip," Nature **42**, 925 (2003).
20. R. Engeln, G. von Helden, G. Berden, and G. Meijer, "Phase shift cavity ring down absorption spectroscopy," Chem. Phys. Lett. **262**, 105 (1996).
21. Z. Tong, A. Wright, T. McCormick, R. Li, R. D. Oleschuk, and H.-P. Loock, "Phase-Shift Fiber-Loop Ring-Down Spectroscopy," Anal. Chem. **76**, 6594 (2004).
22. M. C. Chan and S. H. Yeung, "High-resolution cavity enhanced absorption spectroscopy using phase-sensitive detection," Chem. Phys. Lett. **373**, 100 (2003).
23. J. Rezac, "Properties and applications of whispering-gallery mode resonances in fused silica microspheres," Ph.D. (Oklahoma State University, 2002).
24. A. C. R. Pipino, J. W. Hudgens, and R. E. Huie, "Evanescent wave cavity ring-down spectroscopy with a total-internal-reflection minicavity," Rev Sci Instrum **68**, 2978 (1997).
25. T. J. Kippenberg, "Nonlinear Optics in Ultra-high-Q Whispering-Gallery Optical Microcavities," Ph.D. (California Institute of Technology, 2004).

1. Introduction

Optical microresonators, of different geometries, support ultra-low-loss whispering-gallery modes (WGM) when evanescently excited from adjacent waveguiding structures. These WGM may be understood as rays of light that are guided along the circumference of the resonator by total internal reflection. As expected for any resonantly excited optical cavity, a transfer of energy to the resonator may be observed by an increase of the intensity of the scattered light, and a decrease in the light transmitted by the waveguide used for coupling. Spheres, rings, disks, toroids, cylinders and capillaries have all been investigated as resonators over the past several years [1-7]. The high quality factor (Q) and small mode volume associated with WGMs makes these microresonators suitable for numerous optical devices, such as microlasers [8,9] and add-drop elements [10], as well as chemical sensors [11,12]. The latter application is of particular interest in this work.

The interaction of a chemical analyte with a microresonator occurs through the modification of the optical environment of the resonator. An analyte may have two effects on the cavity mode spectrum of the microresonator. If the effective refractive index of the WGM is increased due to the presence of the analyte, as is frequently the case, the mode field volume increases and the cavity spectrum shifts to longer wavelength. [11] In addition, the analyte may also absorb light, which reduces the quality factor of the cavity and broadens the cavity resonance lines. [13,14] Both effects have been used to implement microresonators as chemical sensors. For chemical sensing the measurement of optical absorption is of particular interest, because it is more specific and less influenced by temperature compared to a refractive index measurement. In the past the reduction in the Q-factor has usually been observed by measuring the linewidth of the cavity resonances, but may also be observed in the time domain using cavity-ring-down spectroscopy (CRD) [15].

Time-domain measurements have been routinely used to measure optical lifetimes in mirror optical cavities [16], as well as in monolithic devices [17], fiber-optic loops [18] and microresonators [8,19]. The intensity of a short optical pulse injected into the cavity decays exponentially with time as the circulating power is dissipated. The time-constant for the decay reflects the optical lifetime of the cavity. While this method is practical for macroscopic cavities, the photon lifetime of microcavities is frequently on the order of nanoseconds requiring picosecond laser pulses and fast data acquisition systems. This will not only increase the cost but also result in a low duty cycle.

An alternative approach to time-domain measurements uses light from an intensity-modulated continuous-wave source. The finite optical lifetime of the resonator induces a phase-shift between the light exiting the cavity and the incident light. The variation in the phase-shift with modulation frequency can be related to the optical lifetime [20]. This phase-shift ring-down approach has been extensively applied to fiber-optic loops [21] and mirror cavities [22]. By applying the robust, inexpensive and simple phase shift CRD method to whispering gallery modes of a microresonator sphere we take a first step to a chemical sensor, which is suited to absorption detection of very small amounts of analyte.

#95586 - $15.00 USD Received 30 Apr 2008; revised 8 Aug 2008; accepted 11 Aug 2008; published 13 Aug 2008

In this work we apply the phase-shift approach to determine the optical loss of microresonator whispering-gallery modes, both in transmission and in scattering mode. A theoretical relationship between the observed phase-shift, the modulation frequency and the microresonator loss parameters is derived using a simple mirror ring-resonator model. As will be shown below, the model is readily transferable to the mirrored cavities typical for phase-shift CRD setups.

2. Experimental

The microresonator used is this work consists of a silica microsphere formed by fusing the end of a single-mode optical fiber in the arc of a fusion splicer. Surface tension draws the molten silica into a sphere with a nominal diameter of 300 μm. The residual fiber supporting the sphere is placed in a fiber chuck that is held in an X-Y-Z stage to allow positioning of the sphere. A tapered single-mode optical fiber, with a waist diameter of 3-4 μm, is used to evanescently couple to the WGMs of the microsphere. The taper is formed by clamping a stripped and cleaned length of single-mode fiber between two motorized translational stages that move in opposition. The fiber is softened in a propane/air flame while the stages separate by a distance of approximately 2 cm. After tapering, the fiber is too fragile for further manipulation. To allow removal of the fiber from the tapering fixture, drops of wax are used to secure the stretched fiber to a microscope slide. An optical microscope is used to measure the taper diameter. The mounted taper is secured to a stage adjacent to the microsphere X-Y-Z stage and the microsphere is carefully brought into contact with the tapered region of the fiber. Optical contact can be easily determined by shining a visible diode laser through the delivery fiber. The microsphere scatters brightly when contact is made with the fiber taper.

An Ando AQ4320D tunable diode laser is used as the excitation light source. The laser is continuously tunable from 1520-1620 nm with a quoted line width of less than 1 MHz. The diode laser intensity is sinusoidally modulated externally using a JDS Uniphase Mach-Zehnder modulator. Unfortunately, the maximum modulation frequency is presently limited to 2 MHz by the function generator (Dae Shin DOA-141). The Mach-Zehnder Interferometer was biased such that the contribution of frequency modulation (FM) was minimized. FM manifests itself in the intensity spectrum through asymmetric lineshapes (see Section 3 below). When examining the WGMs in transmission mode, a D400FC InGaAs detector (Thorlabs, Inc.) is used to measure the light intensity passing through the tapered delivery fiber. A Stanford Research Systems Model SR844 lock-in amplifier processes the detector output, providing an intensity and a phase angle measurement referenced to the diode laser modulation. To examine the WGMs in scattering mode, a switchable gain PDA10CS InGaAs detector (Thorlabs, Inc.), attached to a second X-Y-Z stage, is positioned above the microsphere. To enhance light collection efficiency, an anti-reflection coated ball lens is mounted before the detector. The detector output is processed through a second SR844 lock-in to provide scatter intensity and phase data. The lock-in outputs pass through a Measurement Computing PMD-1608FS A/D before being collected on a computer.

To shield the microresonator and fiber taper from contamination, the entire optical setup is placed under a plastic enclosure that is continuously purged with a gentle flow of nitrogen gas.

3. Theory

The behavior of the microsphere is modeled using a 4-mirror ring-resonator proposed by Rezac (see Fig 1).[23] This model can readily be related to the more common 2-mirror cavity that is used in most CRD setups or to a monolithic ring cavity.[24] Rezac derived equations that describe the frequency dependent intensity of light transmitted through a tapered fiber waveguide in contact with a microsphere resonator, whereas we wish to determine the phase-shift in the envelope of an intensity modulated source coupling to the WGMs of the microsphere. In our case, rather than a single frequency electric field coupling to the resonator, an amplitude-modulated (AM) field is required which implies the presence of

#95586 - $15.00 USD Received 30 Apr 2008; revised 8 Aug 2008; accepted 11 Aug 2008; published 13 Aug 2008

frequency sidebands. Using complex notation for the electric field, we can write the incident AM field as

$$\begin{aligned} E_{inc} &= E_0 e^{i\omega t}\left(\sqrt{1-\beta}+i\sqrt{2\beta}\cos\Omega t\right) \\ &= E_0\sqrt{1-\beta}e^{i\omega t}+E_0\sqrt{\frac{\beta}{2}}\left(e^{i(\omega+\Omega)t+\pi/2}+e^{i(\omega-\Omega)t+\pi/2}\right) \end{aligned} \tag{1}$$

Where β is the modulation depth, ω is the carrier frequency and Ω is the amplitude-modulation frequency of the electric field. Note that the intensity is then modulated by 2Ω. The carrier and each frequency sideband will experience their own attenuation and phase-shift (Φ, Φ_+ and Φ_-, respectively) through interaction with the resonator, and the output field will be

$$E_{trans} = E_\omega\sqrt{1-\beta}e^{i(\omega t+\Phi)}+E_{\omega+\Omega}\sqrt{\frac{\beta}{2}}e^{i[(\omega+\Omega)t+\Phi_++\pi/2]}+E_{\omega-\Omega}\sqrt{\frac{\beta}{2}}e^{i[(\omega-\Omega)t+\Phi_-+\pi/2]} \tag{2}$$

The transmitted intensity is given by

$$I_{trans} = \frac{n_{eff}\varepsilon_0 c}{2} \begin{bmatrix} (1-\beta)E_\omega{}^2+\frac{\beta}{2}\left(E_{\omega+\Omega}{}^2+E_{\omega-\Omega}{}^2\right)+ \\ E_\omega E_{\omega+\Omega}\sqrt{2\beta(1-\beta)}\sin\left(-\Omega t+\Phi-\Phi_+\right)+ \\ E_\omega E_{\omega-\Omega}\sqrt{2\beta(1-\beta)}\sin\left(\Omega t+\Phi-\Phi_-\right)+ \\ \beta E_{\omega+\Omega}E_{\omega-\Omega}\cos\left(2\Omega t+\Phi_+-\Phi_-\right) \end{bmatrix} \tag{3}$$

In our case, we only record the signal modulated at 2Ω with the lock-in amplifier and the associated phase-shift of the modulation envelope is given by $(\Phi_+ - \Phi_-)$.

Rezac's formalism can now be used to calculate the phase-shift at each sideband frequency; the difference $(\Phi_+ - \Phi_-)$ yielding the desired modulation envelope phase-shift. [23] In Eq. (1) we assume that the contribution of frequency modulation (FM) is negligible. This is easily verified experimentally. If FM were present, one would observe dispersive-like lineshapes with zero-crossing at the resonance peak as a consequence of the π phase difference between the sidebands. Such "derivative-type" lineshapes were indeed observed in preliminary experiments when the laser was current modulated, and FM contributions were considerable. When using the Mach-Zehnder interferometer no such effect was observed.

The ring-resonator model assumes a single frequency electric field incident upon a multi-mirror ring-cavity (Fig. 1). The input mirror has a field amplitude reflectivity, Γ, while the other mirrors are assumed totally reflective in our model. As the field propagates within the resonator, it experiences a fractional loss of exp(-αL/2) per pass (the intensity loss is exp(-αL) per pass) , where α is the distributed loss coefficient and L is the round-trip path length. The reflected field from the ring-resonator consists of the superposition of the partially reflected incident field and the partially transmitted field inside the resonator. In our case of a fiber coupled microsphere resonator the *reflected* field of this model corresponds to the light *transmitted* through the tapered delivery fiber. The normalized amplitude of the respective field for a single frequency incident field, is given by [23]

$$E = E_{ref} / E_{inc} = \frac{\Gamma - e^{-\alpha L/2}e^{iLk}}{1-\Gamma e^{-\alpha L/2}e^{iLk}} \tag{4}$$

#95586 - $15.00 USD Received 30 Apr 2008; revised 8 Aug 2008; accepted 11 Aug 2008; published 13 Aug 2008

where the wave vector $k = \omega\, n_{eff} / c$. Accordingly the intensity (shown in Fig. 1(a)) is calculated from the absolute square of (4) as

$$I = \frac{\Gamma^2 - 2\Gamma e^{-\alpha L/2}\cos(Lk) + e^{-\alpha L}}{1 - 2\Gamma e^{-\alpha L/2}\cos(Lk) + \Gamma^2 e^{-\alpha L}} \tag{5}$$

To calculate the phase angle associated with the field of (4) the expression is expanded by the complex conjugate of the denominator

$$E = \frac{\Gamma - \left(\Gamma^2 + 1\right)e^{-\alpha L/2}\cos(Lk) + \Gamma e^{-\alpha L} + i(\Gamma^2 - 1)e^{-\alpha L/2}\sin(Lk)}{1 - 2\,\Gamma\, e^{-\alpha L/2}\cos(Lk) + \Gamma^2 e^{-\alpha L}} \tag{6}$$

With this expression the phase angle associated with the field of (4) is readily described in the complex plane as

$$\begin{aligned}\tan\phi &= \frac{\mathrm{Im}(E)}{\mathrm{Re}(E)} \\ &= \frac{\left(\Gamma^2 - 1\right)e^{-\alpha L/2}\sin(Lk)}{\Gamma - \left(\Gamma^2 + 1\right)e^{-\alpha L/2}\cos(Lk) + \Gamma e^{-\alpha L}}\end{aligned} \tag{7}$$

The phase-shifts at the two sideband frequencies Φ_+ and Φ_- can be calculated from Eq. (7) by using $k_+ = (\omega + \Omega)\, n_{eff}/c$ and $k_- = (\omega - \Omega)\, n_{eff}/c$ respectively.

It is helpful to distinguish different coupling regimes before examining the implications of the above expressions. When $-2\ln\Gamma > \alpha L$, the cavity is 'overcoupled'. In this regime, coupling to the fiber is the dominant loss mechanism controlling the resonance linewidth [25]. When $-2\ln\Gamma < \alpha L$, the cavity is referred to as 'undercoupled', and 'critically coupled' when $-2\ln\Gamma = \alpha L$. At the point of critical coupling, no light is transmitted through the delivery fiber on resonance. Plots of the phase angle obtained from Eq. (7) are shown in Figure 1B for different values of α and assuming $\Gamma = 0.9995$ and $L = 1$ mm. It is apparent that for the undercoupled case the slope is negative in the vicinity of the resonance, and that the magnitude of the slope increases with decreasing loss α. The phase-shift for an intensity-modulated input is given by the difference in the phase angles associated with the sideband frequencies (Eq. (3)). In our experiments the modulation frequency is $<10^{-8}$ of the carrier frequency, and we can simplify

$$(\Phi_+ - \Phi_-) = \frac{2\Omega n_{eff} L}{c}\frac{\partial\Phi}{\partial Lk} \tag{8}$$

Based on Eq. (8), one would expect to observe a phase-shift that varies linearly with modulation frequency, having a slope that increases with decreasing loss in the resonator. When operating near resonance, it is possible to use small angle approximations for the trigonometric functions in Eq. (7) and obtain the result

$$\Delta\Phi = \Phi_+ - \Phi_- \approx \frac{-2\Omega n_{eff} L}{c}\frac{x(1-\Gamma^2)}{\Gamma(1+x^2) - x(1+\Gamma^2)} \tag{9}$$

where $x = e^{-\alpha L/2}$. This may also be expressed as

$$\Delta\Phi = \Phi_+ - \Phi_- \approx -\frac{2\Omega n_{eff} L}{c}\frac{2\ln(\Gamma)}{(\ln\Gamma)^2 - (\alpha L/2)^2} \tag{10}$$

#95586 - $15.00 USD Received 30 Apr 2008; revised 8 Aug 2008; accepted 11 Aug 2008; published 13 Aug 2008

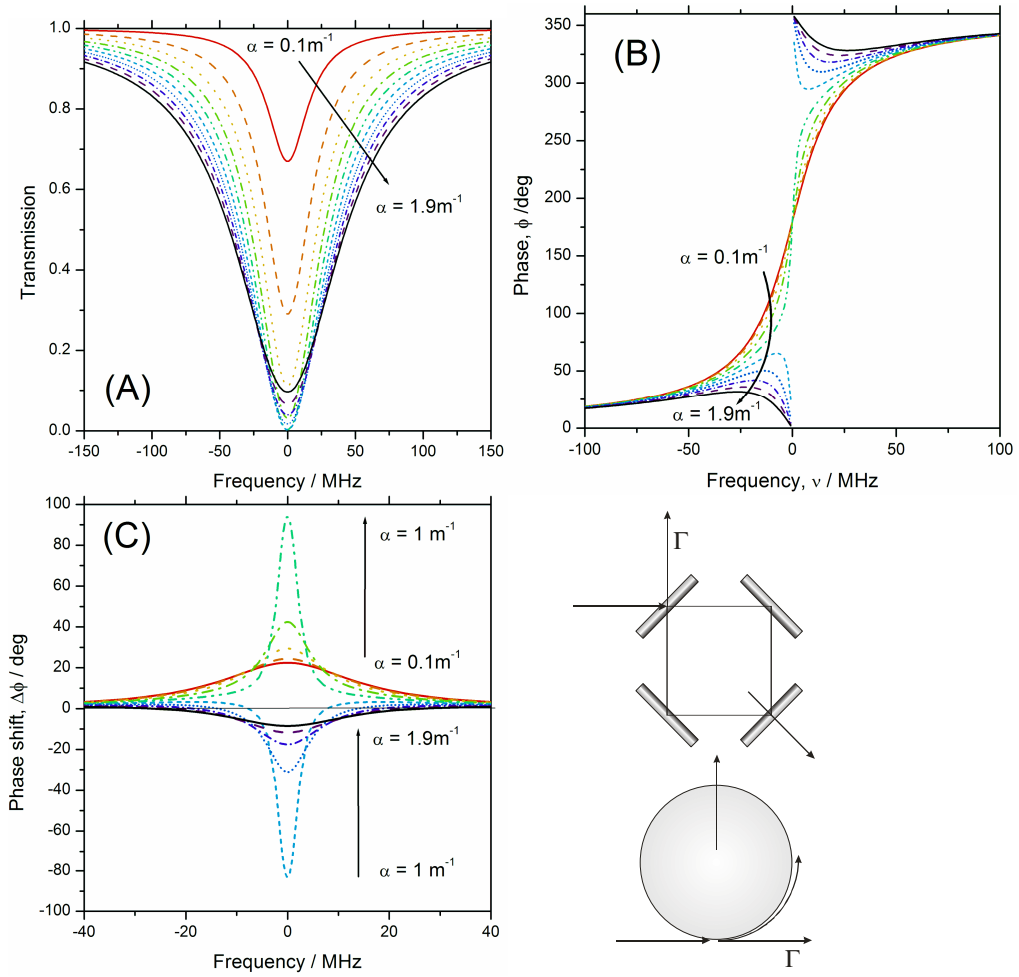

Fig. 1. (a) Intensity of the transmission through the waveguide near a resonance (Eq. (5)). (b) the phase near that resonance calculated from Eq. (7) (c) The corresponding phase-shift spectrum from Eq. (8). For all calculations the absorption coefficient α was varied in 10 increments between 0.1 - 1.9 m^{-1} ($\alpha_{critical}$ = 1 m^{-1}) and the following set of parameters was used: coupling parameter Γ = 0.9995, n_{eff} = 1.45; L = 1 mm; ω = 2 10^{14} s^{-1}.

Equation (9) and (10) explicitly relate the phase-shift to the modulation frequency and loss within the microresonator. Equation (10) shows that the phase-shift is negative in the case of an undercoupled excitation and positive if the resonator is operated in the overcoupled regime. This is also illustrated in Fig. 1(c), where it is apparent that the phase-shift switches abruptly from positive to negative as α is increased from the undercoupled to the overcoupled case. From (10) it is apparent that the phase-shift increases linearly with increasing modulation frequency Ω, and with decreasing dB loss. As can be shown, the resonance line width decreases accordingly.

In the case of scattered light, we need only concern ourselves with the field circulating within the microresonator. This case is very similar to those described in the cavity ring-down literature for an optical cavity with two or more mirrors. The intensity of resonant light circulating within the cavity will decay exponentially over time, with a lifetime given by

$$\tau = \frac{n_{eff} L}{c(-\ln \Gamma^2 + \alpha L)} \tag{11}$$

#95586 - $15.00 USD Received 30 Apr 2008; revised 8 Aug 2008; accepted 11 Aug 2008; published 13 Aug 2008

In our experiment intensity modulated light is injected into the microresonator. From the field in Eq. (1) the intensity is [20]

$$I(\omega,t) = E_0^2(\omega)\left(1+\beta\cos(2\Omega t)\right) \tag{12}$$

where $0 \le \beta \le 1$ is the modulation depth. The intensity, $E_0^2(\omega)$, is dictated by the WGM spectrum. The intensity of light scattered from the microresonator at time *t* is given by [20]

$$\begin{aligned} I(\omega,t) &= \frac{1}{\tau}\int_{-\infty}^{t} E_0^2(\omega)\left(1+\beta\cos(2\Omega t')\right)\exp\left[-\frac{(t-t')}{\tau}\right]dt' \\ &= E_0^2(\omega)\left(1+\frac{\beta}{\sqrt{1+4\Omega^2\tau^2}}\cos\left(2\Omega t-\tan^{-1}(2\Omega\tau)\right)\right) \end{aligned} \tag{13}$$

From this expression we can see that the scattered light is phase-shifted with respect to the input light by an amount

$$\begin{aligned} \Delta\Phi &= -\tan^{-1}(2\Omega\tau) \\ &\approx -2\Omega\tau \\ &\approx -\frac{2\Omega n_{eff} L}{c}\frac{1}{-2\ln\Gamma+\alpha L} \end{aligned} \tag{14}$$

for small phase-shifts. Note that the phase-shifts described by Eqs. (14) and (10) are different especially with respect to the sign of the coupling parameter Γ, i.e. only in Eq. (14) is Γ contributing to the optical loss.

As shown in (13) the depth of the modulation amplitude is also dependent on Ω and τ but since Ωτ<<1 this contribution can be neglected and the intensity $I(\omega)$ is proportional to the measured quantity $\beta I_0(\omega)$. Similarly, in deriving Eq. (5) for the intensity of the transmitted light, we also assumed that the angular modulation period is long compared to the WGM ring-down time.

4. Results and discussion

Figure 2 shows whispering-gallery mode intensity spectra for a ~300 μm diameter silica microsphere obtained in transmission and in scattering mode. An obvious high degree of correlation exists between these two spectra, as would be expected. Based on the linewidth of non-overlapped peaks, the loaded Q-factor for this resonator is ~10^6. A perfectly spherical resonator exhibits a high degree of mode degeneracy that leads to a relatively sparse and regular WGM spectrum. Departure from this ideal case lifts the degeneracy, leading to the complicated and congested cavity mode spectrum seen in Fig. 2. Figure 3 displays the phase-shift spectra for WGMs, observed in transmission mode (Fig. 3(a)) and scattering mode (Fig. 3(b)), and measured at 1.6 MHz modulation frequency. For the scattered light negative phase-shifts are always measured, as predicted by theory, whereas for the transmitted light the sign of the phase-shift was found to be strongly dependent on the mode. The spectrum shown in Fig. 3(a) is representative for the undercoupled regime, but other spectra (Figure 4) show sharp positive *and* negative peaks, which both correspond to minima in the transmission intensity spectrum. A large variation in phase-shift exists from mode to mode. This reflects variation in the input coupling efficiency (Γ) and loss (αL) among the various resonator modes. As predicted from the model the peaks in the phase-shift spectra are narrower than those in the intensity spectra and their peak widths were found to decrease with increasing modulation frequency. The congested mode spectrum for an aspherical microresonator results in considerable spectral overlap, as can be seen in the intensity spectra of Fig. 3(a) and (b) overlap. The overlap is somewhat reduced for the more narrow peaks in the phase-shift spectra. For example, peak "b" in Fig. 3(b) shows a sharp resonance in the phase-shift spectrum but only appears as a shoulder in the scattering intensity spectrum.

#95586 - $15.00 USD Received 30 Apr 2008; revised 8 Aug 2008; accepted 11 Aug 2008; published 13 Aug 2008

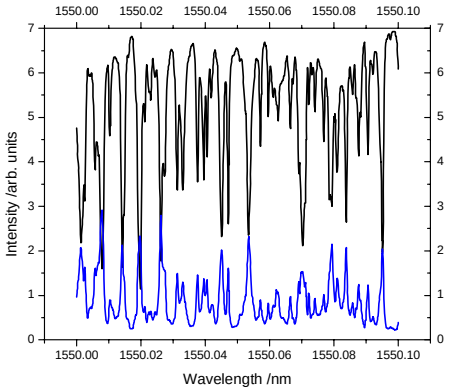

Fig. 2. Whispering-gallery mode spectrum of a 300 micron diameter silica microsphere in contact with a 3 micron diameter tapered fiber. Spectra are recorded in transmission (top) and in scattering mode (bottom).

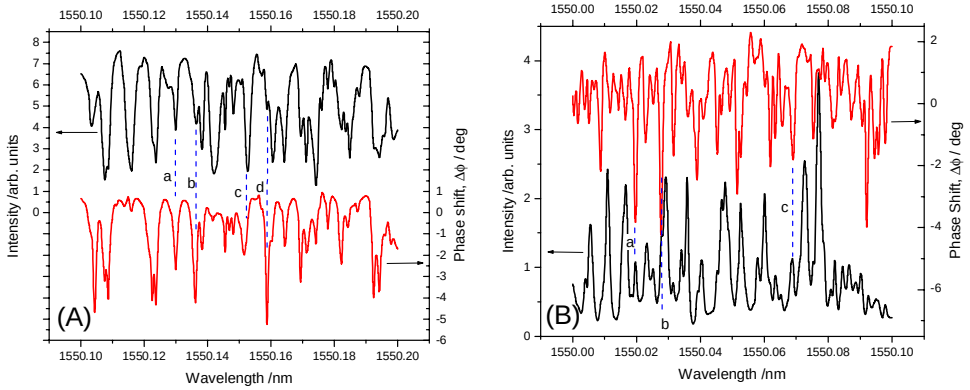

Fig. 3. Phase-shift spectrum and intensity spectra of a 300 μm diameter microsphere. (a) The measurement was conducted by detecting the light transmitted through the fiber taper. (b) Scattered light was collected above the microsphere. The modulation frequency is 1.6 MHz.

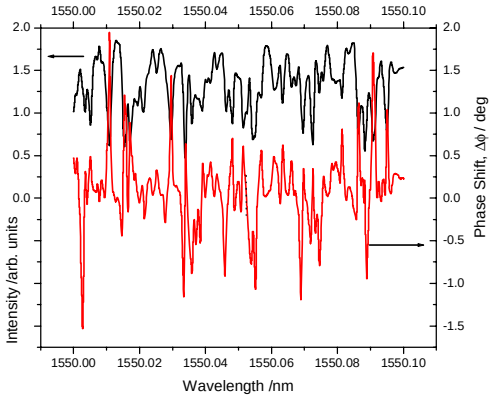

Fig. 4. Transmitted light (upper trace) and phase angle WGM spectrum of the microsphere. The phase-shift CRD spectra show that some of the WGMs are overcoupled (positive going peaks) whereas others are undercoupled (negative).

#95586 - $15.00 USD Received 30 Apr 2008; revised 8 Aug 2008; accepted 11 Aug 2008; published 13 Aug 2008

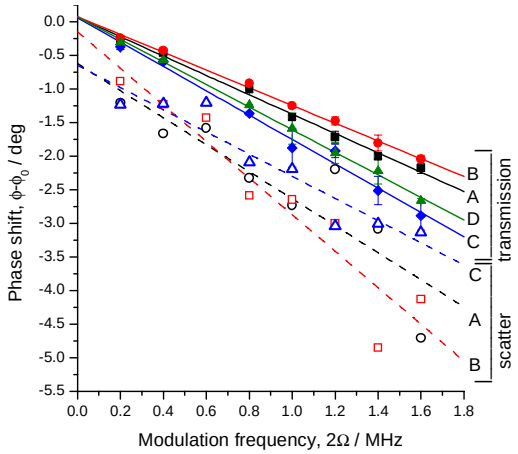

Fig. 5. Modulation frequency dependent phase-shift for the four peaks shown in the transmission spectrum (solid lines and symbols, see Fig. 3(a)) and the three peaks shown in the scattering spectrum (dashed, empty symbols, Fig. 3(b) From the former the slopes of the linear fits can be used to calculate the parameter $2\ln\Gamma/\left[(\ln\Gamma)^2-(\alpha L/2)^2\right]$ as 757, 829, 962, 1039, respectively (see Eq. (10)). Ring-down times of 5.6, 7.5 and 4.6 ns are obtained directly from the slope of linear fits of the modulation frequency dependent phase-shift for peaks A, B and C in the scattering spectrum.

The scattering peak amplitudes in the phase-shift and in the intensity spectra are not expected to be similar (Fig. 3(b)). In the scattering intensity spectrum the amplitude represents the power coupled into the respective mode, i.e. a quantity that depends on the square of the ring-down time, whereas in the phase-shift spectrum the peak amplitude scales linearly with the ring-down time. Also, the scattering intensity is easily influenced by a background arising e.g. from scattering off the tapered waveguide. By contrast, a large change in phase shift can only arise from a WGM with a long decay time. Since the decay time is strongly affected by the presence of analytes on the microresonator surface, the phase-shift measurement may be more robust, albeit less sensitive, compared to an intensity or linewidth measurement.

The transmission peak amplitudes in the phase shift and intensity spectra (Fig. 3(a)) are also not well correlated, since the phase-shift is much more strongly dependent on the coupling regime compared to the intensity. The most pronounced peaks in the transmission phase-shift spectrum correspond to WGM which experience near critical coupling conditions.

Figure 5 displays the modulation frequency dependence of the measured *scattering* phase angle for resonant excitation of three different modes corresponding to non-overlapped peaks in the respective spectra (Fig. 3). The phase angle measurements have a considerable measurement error due to the low light level emitted by the high-Q resonator, but with eq. (14) nevertheless give reasonable estimates of the ring-down times as τ = 4 - 8 ns. For these three modes the quality (Q) factor is therefore between about 5 10^6 and 10 10^6. With an estimated sphere circumference of 1 mm and assuming a refractive index of 1.45 the loss per roundtrip is calculated to be between 0.0025 dB and 0.005 dB. The propagation loss of 2.5 - 5.0 dB/m for these WGMs compares poorly to losses achieved in single mode waveguides made from the same silica material (3 dB/km), but is comparable to propagation losses achieved in some microtoroidal resonators (0.5 dB/m) [19].

Also included in Fig. 5 is the modulation frequency dependence of the *transmission* phase angle given at the resonance peak of four modes (*viz*. Fig. 3). A linear relationship, with negative slope, is observed as predicted by Eq. (10) for the undercoupled regime. The differences in slope are due to differences in coupling efficiency and/or optical loss. For the overcoupled regime the model predicts a positive phase-shift and slope. Very close to critical coupling the model presented in Eq. (10) breaks down and it can be shown that the respective

#95586 - $15.00 USD Received 30 Apr 2008; revised 8 Aug 2008; accepted 11 Aug 2008; published 13 Aug 2008

graphs then deviate from linearity. Given the total loss calculated from the scattering phase-shift one obtains $\Gamma_{critical} = 0.9998$ and $\alpha_{critical} = 0.43\ m^{-1}$. As can be seen in Fig. 4 we operated very close to critical coupling conditions, since both undercoupled and overcoupled WGMs could be observed.

5. Summary and conclusion

The phase-shift CRD technique is a simple and inexpensive method to measure ring-down times of whispering gallery modes in the nanosecond range or even lower. Measurement of such a short ring-down time in the time-domain would require expensive picosecond laser sources and fast data acquisition systems whereas the same information is readily obtained with standard inexpensive telecom instrumentation through phase-shift measurements at two or more different modulation frequencies. As can be seen from the model developed in this report, even shorter ring-down times maybe measured with high accuracy using modulation frequencies in the 10-100 MHz regime. Complementary information is available from measurements of light scattered by the microresonator and from light that is allowed to interfere with incoming light - here the light transmitted by the waveguide, which was used to couple light into the resonator. The phase-shift of the scattered light scales inversely with the total dB loss in the resonator, whereas the phase-shift of the transmitted light is maximized for near critical coupling conditions. In the overcoupled (undercoupled) regime phase angles were found to be positive (negative) and linearly dependent on the modulation frequency. Since the scattering measurement is biased towards low loss WGMs, this method may prove useful to interrogate microresonators in chemical sensing applications. The detection limit offered by interrogating microsphere resonators with phase-shift CRD, may be estimated from the present precision of the optical loss measurements. Assuming conservatively that a change of 0.5 degrees at a modulation frequency of 1.6 MHz can be measured, we expect to resolve a change from $\alpha = 0.2\ m^{-1}$ to $0.3\ m^{-1}$. For strong absorption features, with absorption coefficients in the order of 10,000 L mol^{-1} cm^{-1}, we then may be able to detect concentrations as low as 10^{-7} M, if the entire mode is exposed to the analyte. Given that the evanescent tail of the WGM only contributes a few percent to the mode field volume, the limit of detection is higher by the corresponding ratio of WGM field volume and evanescent wave volume.

Acknowledgments

We thank Photonics Research Ontario (Ontario Centres of Excellence) for financial support of this work. Contributions from the Canadian Institute for Photonic Innovations (CIPI), from the Natural Science and Engineering Research Council (NSERC) are acknowledged by the Canadian researchers. GG also acknowledges financial support from the Italian Ministry for Education, University and Research (PON-SIMONA) and assistance from the Consiglio Nazionale delle Ricerche by the RSTL-project and the short term-mobility program.

#95586 - $15.00 USD Received 30 Apr 2008; revised 8 Aug 2008; accepted 11 Aug 2008; published 13 Aug 2008